Cancer Science
Japanese Cancer Association JCA
Open Access

Spread of tumor microenvironment contributes to colonic obstruction through subperitoneal fibroblast activation in colon cancer

Mitsuru Yokota,[1,2] Motohiro Kojima,[3] Youichi Higuchi,[4] Yuji Nishizawa,[1] Akihiro Kobayashi,[1] Masaaki Ito,[1] Norio Saito[1] and Atsushi Ochiai[3]

[1]Division of Colorectal Surgery, Research Center for Innovative Oncology, National Cancer Center Hospital East, Kashiwa; [2]Department of Surgery, School of Medicine, Keio University, Tokyo; [3]Division of Pathology, Research Center for Innovative Oncology, National Cancer Center Hospital East, Kashiwa; [4]Laboratory of Cancer Biology, Department of Integrated Biosciences, Graduate School of Frontier Sciences, The University of Tokyo, Tokyo, Japan

Key words
Colon cancer, elastic laminal invasion, fibroblast, obstruction, tumor microenvironment

Correspondence
Atsushi Ochiai, Division of Pathology, Research Center for Innovative Oncology, National Cancer Center Hospital East, 6-5-1 Kashiwanoha, Kashiwa 277-8577, Japan.
Tel: +81-4-7133-1111; Fax: +81-4-7131-9960;
E-mail: aochiai@east.ncc.go.jp

Funding Information
Japan Society for the Promotion of Science.

Received November 4, 2014; Revised January 3, 2015; Accepted January 14, 2015

Cancer Sci (2015)

doi: 10.1111/cas.12615

We evaluated the influence of the cancer microenvironment formed by peritoneal invasion (CMPI) on clinical findings in colon cancer patients. In addition to the association with poor prognosis, we discovered a relationship with bowel obstruction. Detailed analysis revealed that clinical findings related to bowel obstruction occurred more frequently in patients with an elevated type tumor, which had peritoneal elastic laminal elevation to the tumor surface, compared to those with non-elevated type tumors among those with elastic laminal invasion (ELI). Lateral tumor spread and increase of tumor annularity rate in ELI-positive elevated type cases suggested the morphological progression from ELI-positive non-elevated type to elevated type. In addition, α-smooth muscle actin expression was the highest in ELI-positive elevated type, and prominent expressions were found not only in the deep tumor area but also in the shallow tumor area. Furthermore, contraction assays revealed the robust contractile ability of subperitoneal fibroblasts stimulated by cancer cell-conditioned medium. Our findings suggest that CMPI spread into the luminal side of the colonic wall along with tumor progression, which caused bowel obstruction through the activation of subperitoneal fibroblasts. However, although the clinical outcome was not different between the two types, the clinical findings were affected by the spread of CMPI. We are the first to explore how the alteration of the tumor-promoting microenvironment, along with tumor progression, contributes to the development of clinical findings.

Colorectal cancer (CRC) is one of the most frequent malignancies in the world.[1–3] The majority of patients with early stage CRC have no symptoms and their cancers are often detected during colorectal screening. However, in spite of the development of the screening system, there are still many patients whose cancers are diagnosed in an advanced stage with clinical findings such as melena, abdominal pain, or obstruction.[4,5] Clinical findings related to CRC are caused by tumor growth into the intestinal lumen and tumor invasion to the adjacent organs, therefore the development of clinical findings typically occurs in relatively advanced stage CRC. Nevertheless, not all patients with advanced stage CRC experience clinical findings. For instance, patients with an apple-core lesion on barium enema examination do not always show obstructive symptoms and there may be no difficulty in passage of the colonoscope despite a typical annular severe stricture formation. Thus, the relationship between clinical findings and tumor progression remains unclear.

Recently, peritoneal elastic laminal invasion (ELI) was reported to be a strong prognostic factor in colon cancer (CC).[6–8] Furthermore, we reported that the cancer microenvironment formed by the peritoneal invasion (CMPI) promoted tumor progression and metastasis through the interaction between subperitoneal fibroblasts (SPFs) and cancer cells.[9] Peritoneal tissue is one of the final layers of the colonic wall, so ELI occurred in advanced stage CC. In addition, marked morphological and pathological alterations were observed in tumor tissues after ELI. Therefore, ELI, and CMPI formed after ELI, may cause CC-related clinical findings. In this study, we aimed to evaluate how the formation of the tumor microenvironment, such as CMPI, could change the characteristics of the tumor tissue, and whether it could affect clinical findings. Using detailed morphometrical and biological investigation, we evaluated the interaction between SPFs and cancer cells within CMPI in colonic obstruction.

Materials and Methods

Patient selection and follow-up. A total of 205 patients with pT3 and pT4a CC who underwent curative surgery at the National Cancer Center Hospital East (Kashiwa, Japan) between January 2007 and December 2010, were retrospectively evaluated (Fig. 1). Demographics, clinical symptoms

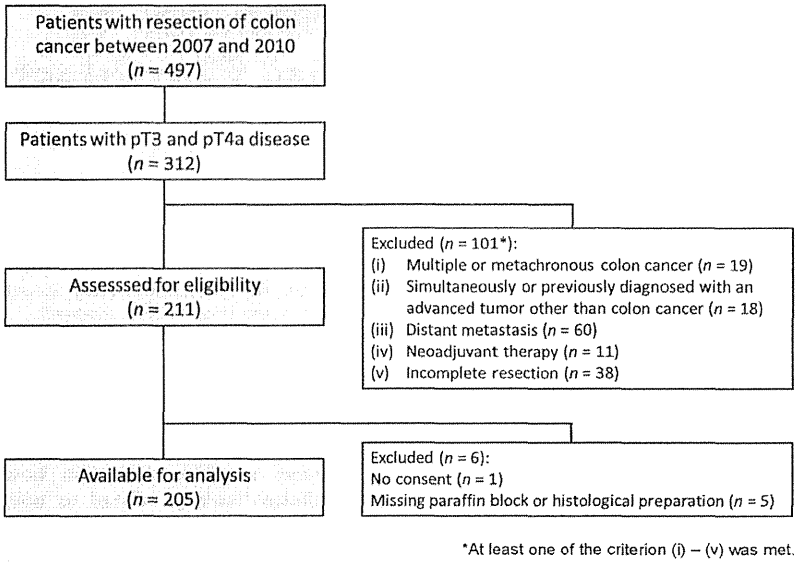

Fig. 1. Flow diagram of the study of colon cancer patients with pT3 and pT4a disease who underwent curative surgery between January 2007 and December 2010. *At least one of the criteria (i–v) was met.

and treatments, serum data, colonoscopy findings, and histopathology and prognostic outcome data for the patients were recorded. Clinical symptoms included abdominal pain, abdominal distension, and vomiting. Treatment of bowel obstruction, including fasting and infusion or decompression with an ileus tube, was carried out according to the severity of the patient's condition. No passage of colonoscope was defined as the inability of an experienced endoscopist to pass a thin scope (φ11.5 mm) beyond a tumor site to the oral-sided colon, and was recorded as one of the features of bowel obstruction.

All cases were reclassified based on the 7th edition of the Union for International Cancer Control TNM staging system.[10] We did not categorize isolated tumor deposits as lymph node metastases to evaluate independently. Follow-up after surgery was carried out in all patients and was comprised

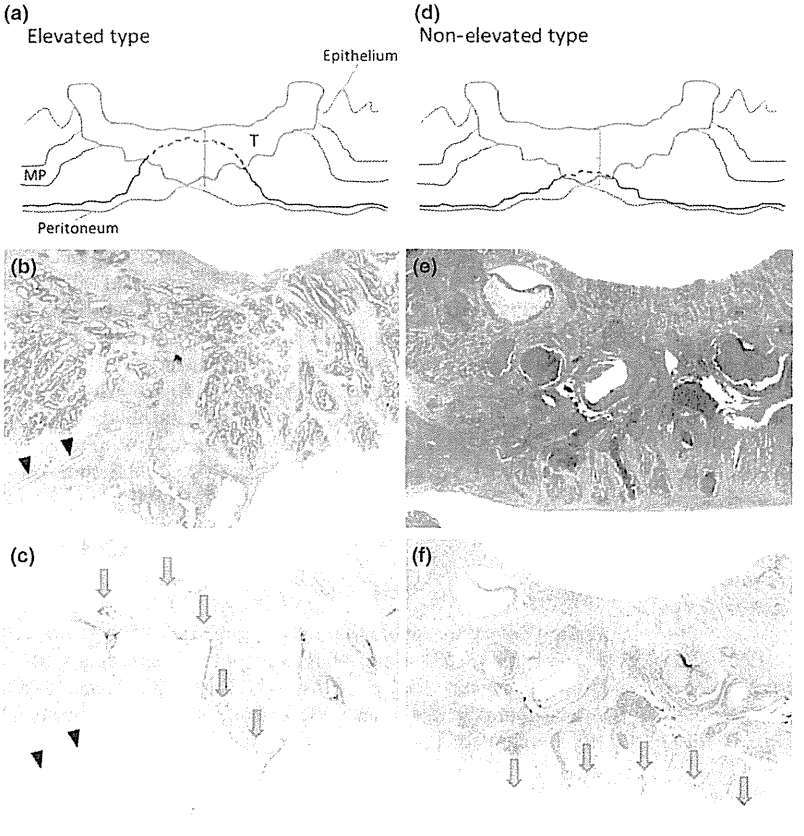

Fig. 2. Two types of elastic lamina invasion (ELI)-positive cases of colon cancer. ELI-positive cases were divided into elevated type (a) and non-elevated type (d) based on whether or not the peritoneal elastic lamina (PEL) was elevated to the surface by more than half the distance of the tumor invasion. H&E staining (b, ×20) and elastica staining (c, ×20) of the elevated type. H&E staining (e, ×20) and elastica staining (f, ×20) of the non-elevated type. Red line represents PEL (a, d). Arrow heads indicate cleft (b, c). Arrows indicate PEL (c, f). MP, muscularis propria; T, tumor.

of serum tumor marker measurement every 3 months and chest and abdominal computed tomography (CT) every 6 months for the first 3 years, then every 6 months for the next 2 years. All patients were followed up from the date of surgery to the last contact (death or last follow-up). Metastasis and local recurrence were considered as tumor recurrence, and the final diagnosis was made by imaging (CT, magnetic resonance imaging, and/or PET-CT), cytology, or biopsy.

Written informed consent for tissue collection and use for research was obtained. The conduct of the study was approved by our local ethics committee (National Cancer Center Hospital; no. 2013-293).

Histopathological analysis. We used the same histopathological examination protocol as that used in our previous study.[6] The resected specimens were fixed in 10% formalin, and the entire tumor was cut into 5-mm slices. Representative slices were embedded in paraffin, cut into 3-μm sections and stained with H&E and elastica stain to evaluate ELI status and lymphovascular invasion. Because of discrimination of the peritoneal elastic lamina (PEL) from the retroperitoneal fascia, we confirmed the continuity from the PEL found at the other area of colonic wall. Therefore, we undertook elastica stain on at least one whole slice where the tumor was closest to the peritoneal surface. The median numbers of H&E and elastica stained sections were 8.0 (range, 2–27) and 5.0 (range, 2–16), respectively.

Cases with tumor invasion beyond the PEL were defined as ELI-positive. First, we divided patients into ELI-positive and ELI-negative cases to identify the difference of clinical features based on the ELI status. Additionally, ELI-positive cases were divided into elevated type or non-elevated type. Cases with the PEL elevation to the surface of more than half the distance of the tumor invasion were regarded as ELI-positive elevated type (Fig. 2). Then, the association between the clinicopathological findings and the three tumor types (ELI-negative, ELI-positive non-elevated type, and ELI-positive elevated type) were assessed.

Azan staining, immunohistochemistry, and computer-assisted image analysis. Two consecutive sections of 4-μm thick slices were obtained from paraffin-embedded blocks, which included all layers of the intestinal wall and tumor area with the deepest infiltration. One section was used for immunohistochemical α-smooth muscle actin (α-SMA) staining (×200, clone 1A4; Dako, Carpinteria, CA, USA) and the other for Azan staining. Immunostaining was carried out using an autostainer (Ventana Benchmark; Roche Diagnostics, Tokyo, Japan), as described previously.[9] High-resolution slide images from each H&E, α-SMA, and Azan stained section were obtained using a Nano Zoomer 2.0-HT slide scanner (Hamamatsu Photonics, Hamamatsu, Japan). All sections were examined using viewer software (NDP View; Hamamatsu Photonics). We divided the tumor area into two equal parts of shallow and deep areas. Five fields with the highest α-SMA and Azan expressions were randomly selected from the shallow and deep layer of each tumor (a total of 10 fields per specimen). Then, images of ×40 magnification (0.59 mm^2) were saved as JPEG files. The ratios of the α-SMA and Azan positive area in the images were calculated using morphometric software (WinRoof; Mitani, Fukui, Japan), as described previously.[9]

Cell cultures and cell lines. Both SPFs and submucosal fibroblasts (SMFs) were obtained from normal sigmoid colon tissue of three patients operated on for sigmoid CC as described previously.[9] The samples were routinely maintained in MF-medium (Toyobo, Tokyo, Japan) at 37°C in a humid atmosphere containing 5% CO_2.

The human colonic cancer cell line DLD-1 was obtained from ATCC (Manassas, VA, USA), and maintained in DMEM (Sigma-Aldrich, St. Louis, MO, USA) containing 100 U/mL penicillin and 100 μg/mL streptomycin (Sigma-Aldrich) and 10% FBS (Gibco, Palo Alto, CA, USA).

Preparation of cancer cell-conditioned medium. Cancer cell-conditioned medium (CCCM) from DLD-1 was obtained as described previously.[9] Initially, $1.7 \times 10^4/cm^2$ of DLD-1 was grown in maintained medium for 48 h, and then starved in DMEM for 24 h. The medium was removed and used as CCCM.

Collagen gel contraction assay. A standard kit assay was used to investigate the difference of contractile ability in fibroblasts (Cell Biolabs, San Diego, CA, USA).[11] Briefly, $1.0 \times 10^5/mm^3$ fibroblasts were mixed with a cold collagen gel solution, then 0.5 mL fibroblast–collagen mixture was added per well in a 24-well plate, and incubated for 1 h at

Table 1. Clinical characteristics according to elastic laminal invasion (ELI) status in patients who underwent primary resection for pT3 and pT4a colon cancer (*n* = 205)

	ELI(−) *n* = 113	ELI(+) *n* = 92	*P*-value
Age, years			
Median (range)	68 (24–90)	64 (38-89)	0.051
Sex			
Male	51	46	0.488
Female	62	46	
Body mass index, kg/m^2			
Median (range)	23.3 (16.2–34.2)	22.5 (14.5–39.3)	0.141
Total protein level, g/dL			
Median (range)	6.8 (5.4–7.9)	6.8 (5.2–7.9)	0.886
Albumin level, g/dL			
Median (range)	4.1 (2.4–4.8)	4.0 (2.7–5.0)	0.821
C-reactive protein level, mg/dL			
Median (range)	0.10 (0.01–6.46)	0.12 (0.01–5.10)	0.867
White blood cell count, /mm^3			
Median (range)	5700 (3200–11 800)	5850 (3200–12 000)	0.571
Neutrophil count, /mm^3			
Median (range)	3429 (1728–8626)	3485 (1141–9821)	0.551
Lymphocyte count, /mm^3			
Median (range)	1693 (776–3493)	1736 (773–5064)	0.758
Hemoglobin concentration, g/dL			
Median (range)	12.7 (6.9–17.7)	12.7 (7.6–16.7)	0.712
CEA level, ng/mL			
Median (range)	3.6 (0.6–358.9)	3.4 (0.7–197.0)	0.401
Tumor location			
Right	40	22	0.193
Transverse	17	18	
Left	56	52	
Abdominal symptoms			
+	25	34	0.020
−	88	58	
Passage of colon colonoscope†			
+	91	50	<0.001
−	19	41	
Treatment of bowel obstruction			
+	2	11	0.003
−	111	81	

CEA, carcinoembryonic antigen. †Four patients were missing data.

37°C. After the gel polymerization, 1 mL DMEM containing 100 U/mL penicillin, 100 μg/mL streptomycin, and 10% FBS was added and incubated for 24 h. Next, the medium was removed from the plate, and CCCM was added to three wells of each fibroblast type. As a control, serum-free DMEM was added to another three wells. Twenty-four hours later, each gel was gently released from the sides of wells, and pictures were taken another 48 h later. The area of the gel was measured using morphometric software (WinRoof; Mitani), and the contraction rate was obtained by the division of the gel area with CCCM stimulation by the initial gel area.

Statistical analysis. Differences in the clinicopathological features between ELI-positive and ELI-negative cases were assessed using Fisher's exact test and the Mann–Whitney *U*-test; α-SMA and Azan positive area ratios were compared using Student's *t*-test.

Recurrence-free survival (RFS) was defined as the time that elapsed between the date of surgery and any relapse or the last contact. Kaplan–Meier survival curves were plotted and compared using the log–rank test.

All statistical analyses were carried out using SPSS 22 (SPSS, Chicago, IL, USA). All *P*-values were reported as two sided, and statistical significance was defined as $P < 0.05$.

Results

Association between clinical characteristics and ELI status. In the dataset, 92 patients (44.9%) were identified as ELI-positive. Serum data, nutritional status, level of tumor marker, and tumor location were not associated with ELI status (Table 1). However, patients with ELI-positive tumors more frequently complained of clinical symptoms and required treatment for bowel obstruction. No passage of the colonoscope was also found more frequently in ELI-positive cases. For a detailed analysis, dividing ELI-positive cases into two types, clinical findings related to bowel obstruction were found more frequently in the ELI-positive elevated type than in the ELI-positive non-elevated type cases (Fig. 3). Furthermore, patients with ELI-positive elevated type tumors required more treatment for bowel obstruction compared to patients with ELI-negative or ELI-positive non-elevated type tumors.

Association between histopathological characteristics and ELI status. Thirty-eight percent of patients with pT3 disease ($n = 70$) and all patients with pT4a disease ($n = 22$) were ELI-positive. Histopathological findings by tumor type are shown in Table 2. Thin ulcers and thickening under the muscular layer were identified as morphological changes associated with an ELI-positive state. The ELI-positive type was also significantly associated with an invasive infiltrating pattern, a higher pathological nodal stage, a high budding grade, a high lymphovascular invasion grade, and a high perineural invasion grade; features that are related to tumor malignancy. Furthermore, tumor size and annularity rate significantly increased in the ELI-positive elevated type cases. These clinicopathological results suggested that elevation of PEL was associated with bowel obstruction and occurred in parallel with tumor progression.

Association between fibrosis and ELI status. Fibrosis in CRC is associated with bowel obstruction.[12–14] Therefore, we quantitatively assessed fibrosis in tumor tissue using morphometry on Azan and α-SMA staining, which was evaluated by tumor type.

The α-SMA expression was higher in order of ELI-positive elevated type, ELI-positive non-elevated type, and ELI-negative

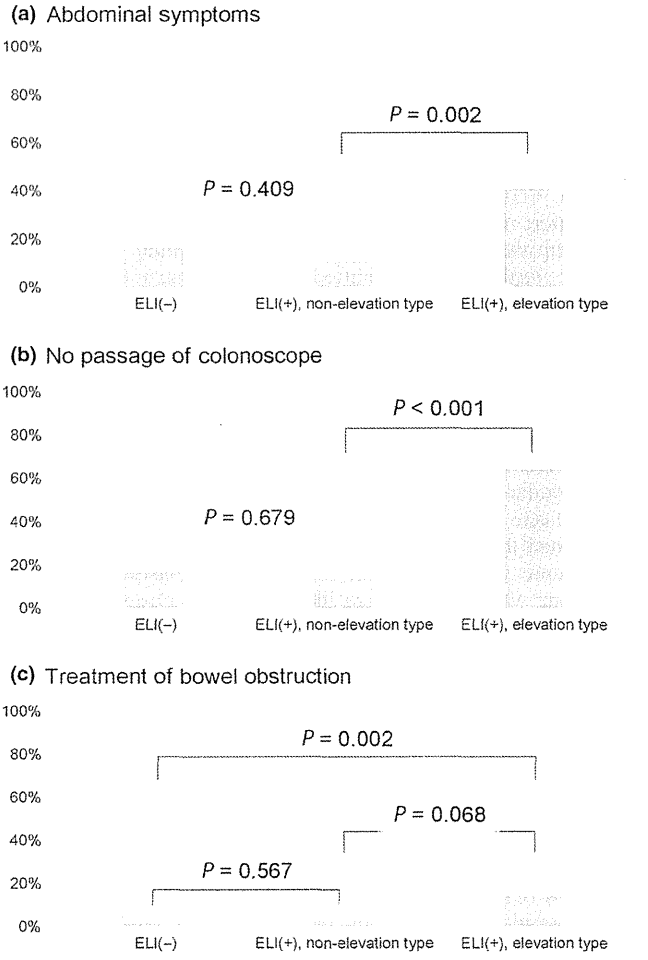

Fig. 3. Incidence rates of clinical findings by colon cancer tumor type. Clinical findings included abdominal symptoms (a), no passage of the colonoscope (b), and treatment of bowel obstruction (c). Tumor types were divided into elastic lamina invasion (ELI)-negative type, elevated type ELI-positive cases, and non-elevated type ELI-positive cases.

cases (Fig. 4a,b). An increase of α-SMA positive area ratio was strongly associated with ELI status, and it was observed not only in the deep tumor area but also in the shallow tumor area. Furthermore, there was a significant difference in the ratio between ELI-positive elevated type and ELI-positive non-elevated type, especially in the shallow tumor area. In the Azan stain, the fibrosis area was also higher in ELI-positive cases than in ELI-negative cases, but the ratio was not different between ELI-positive elevated type and ELI-positive non-elevated type (Fig. 4a,c).

Association between prognosis and ELI status. The median follow-up was 4.3 years (range, 0.3–6.6 years). The 3-year RFS rates for ELI-negative and ELI-positive patients were 95.4% and 74.9%, respectively, and the log–rank analysis revealed a statistically significant difference ($P < 0.001$; Fig. 5a). However, the 3-year RFS rates for ELI-positive non-elevated type and ELI-positive elevated type were 72.2% and 76.7%, respectively, and there was no significant difference between these two types among ELI-positive patients ($P = 0.340$; Fig. 5b).

Contractile ability of SPFs. To estimate the contribution of SPFs to bowel obstruction, contraction assays were carried out and contractile abilities were compared with those of SMFs.

Table 2. Clinical and histopathological findings by tumor type in patients who underwent primary resection for pT3 and pT4a colon cancer ($n = 205$)

	1. ELI(−) $n = 113$	2. ELI(+) Non-elevated type $n = 36$	3. ELI(+) Elevated type $n = 56$	*P*-value (1. *vs* 2.)	*P*-value (2. *vs* 3.)
Maximum transverse tumor size, cm					
Median (range)	4.0 (1.0–10.0)	3.4 (1.0–9.2)	5.0 (2.0–10.5)	0.250	0.003
Maximum longitudinal tumor size, cm					
Median (range)	3.5 (1.0–10.0)	3.0 (1.5–8.0)	4.0 (2.0–8.0)	0.153	0.021
Tumor annularity rate, %					
Median (range)	63.3 (17.6–100)	53.3 (18.8–100)	100 (28.6–100)	0.512	<0.001
Thickness of ulcer, mm					
Median (range)	12.0 (4.0–41.0)	8.0 (4.0–40.0)	9.56 (3.0–26.0)	0.001	0.352
Thickness under the muscular layer, mm					
Median (range)	2.5 (0.1–19.0)	3.0 (0.75–46.0)	4.4 (0.25–20.0)	0.058	0.331
Histologic differentiation					
Well/moderately	108	33	54	0.298	0.298
Poorly/mucinous	5	3	2		
Infiltrating pattern					
Expanding	55	4	4	<0.001	0.382
Invasive	58	32	52		
Tumor depth					
pT3	113	26	44	<0.001	0.486
pT4a	0	10	12		
Nodal status					
pN0	66	16	24	0.002	0.668
pN1	43	12	23		
pN2	4	8	9		
Budding grade					
Grade 1	87	20	35	0.041	0.187
Grade 2	18	12	10		
Grade 3	8	4	11		
Tumor deposits					
+	11	6	6	0.197	0.301
−	102	30	50		
Lymphatic invasion					
+	50	24	37	0.019	0.953
−	63	12	19		
Vascular invasion					
+	64	27	37	0.049	0.364
−	49	9	19		
Perineural invasion					
+	24	15	20	0.015	0.566
−	89	21	36		

ELI, elastic laminal invasion.

The response to CCCM stimulation was significantly higher in SPFs than in SMFs (Fig. 6).

Discussion

In this study, we investigated two types of ELI-positive tumors and first detected the progression-dependent elevation of PEL that was associated with bowel obstruction. Elevation of PEL implied a spread of CMPI toward the luminal surface, and further investigation suggested that the activation of SPFs, which normally reside in the subperitoneal outer area of the colonic wall, contributes to obstruction of the bowel. We have reported that CMPI contributes to tumor progression and metastasis through the interaction of SPFs and cancer cells. Tumors were known to form heterogeneous microenvironments and some of these, including CMPI, promote tumor progression and metastasis.[15–18] However, a progression-dependent alteration of such a tumor microenvironment has not been investigated. In this study, we revealed that a progression-dependent spread of the tumor microenvironment to the shallow layer of the tumor tissue resulted in reduced bowel patency. Our findings first suggest that the tumor-promoting microenvironment can contribute not only to tumor progression or metastasis, but also to the deterioration of clinical findings.

The cancer microenvironment consists of a heterogeneous type of stromal cells, and fibroblasts are one of the major sources.[19] Subperitoneal fibroblasts were reported to be sensitive to CCCM stimulation, and the upregulation of contraction-associated genes, including α-*SMA*, by CCCM was one of the specific features of SPFs.[9] An increase in α-SMA expres-

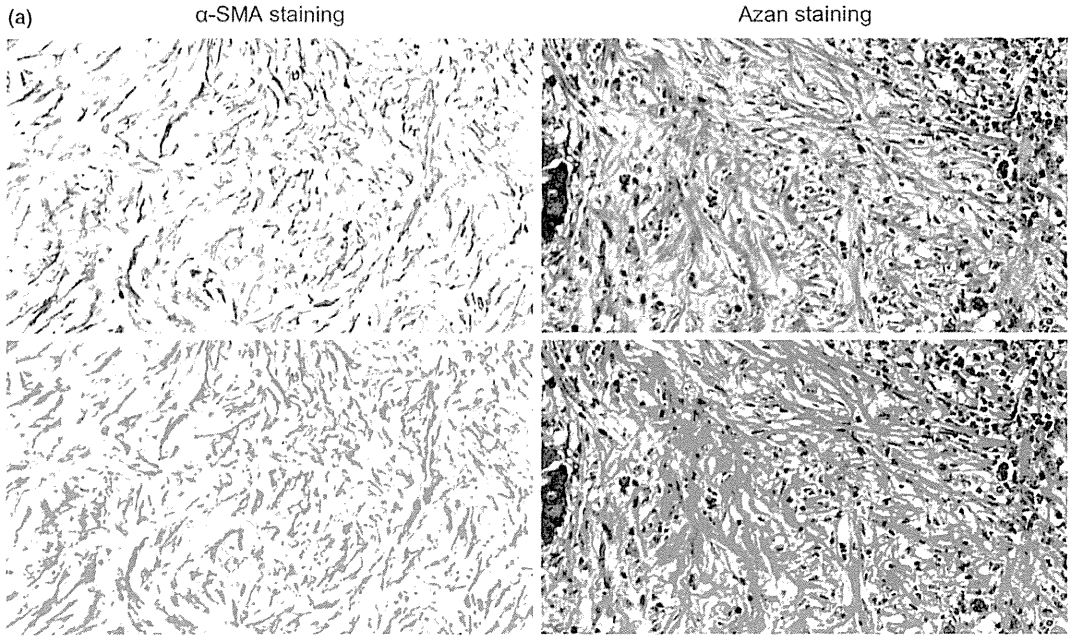

(b) α-SMA staining positive area ratio

Layer	ELI(−)	ELI (+)	
		Non-elevated type	Elevated type
Shallow	11.91% (5.98)	17.68% (5.05)	20.87% (7.05)
Deep	17.68% (6.27)	26.55% (8.89)	28.90% (7.32)
All	14.79% (5.11)	22.11% (5.51)	24.88% (6.02)

(c) Azan staining positive area ratio

Layer	ELI(−)	ELI (+)	
		Non-elevated type	Elevated type
Shallow	32.91% (12.87)	43.83% (14.85)	44.19% (14.20)
Deep	42.24% (11.49)	51.37% (11.64)	50.82% (11.26)
All	37.58% (9.81)	47.60% (11.31)	47.51% (10.88)

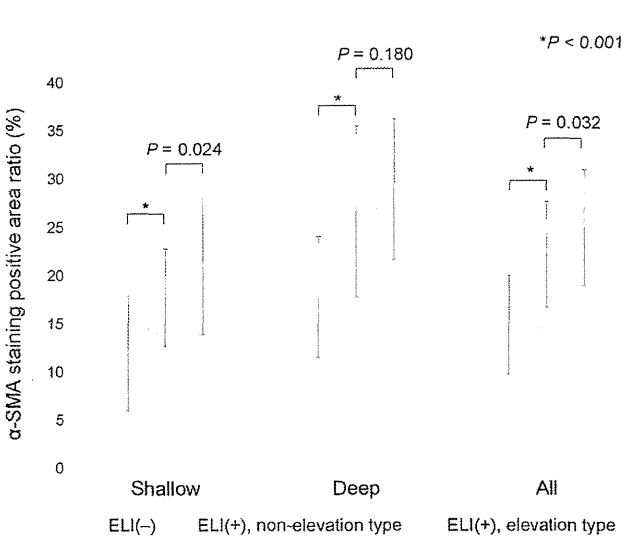

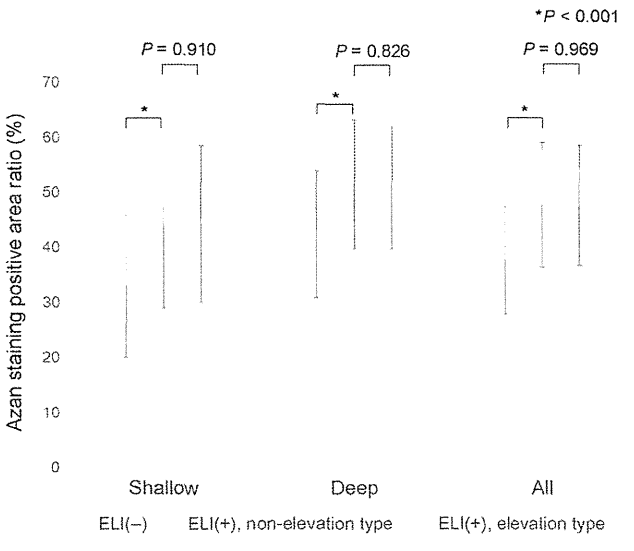

Fig. 4. Association between fibrosis and colon cancer tumor type. α-Smooth muscle actin (α-SMA) staining (×40) and Azan staining (×40) positive areas were successfully detected using morphometric software (a). The α-SMA staining positive area ratio is shown by tumor area (shallow layer, deep layer, and both layers [All]) (b). The Azan staining positive area ratio is also shown (c). Values are mean percentages and those in parentheses are standard deviation. *$P < 0.001$.

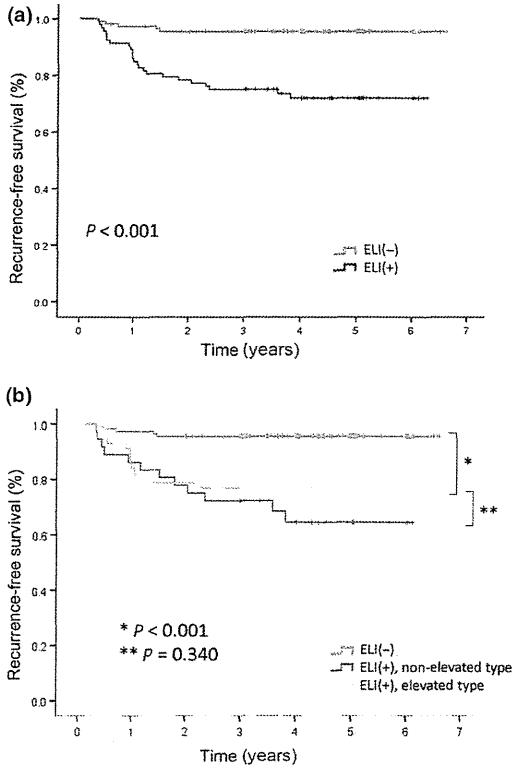

Fig. 5. Kaplan–Meier curves depicting recurrence-free survival of 205 patients who underwent primary resection for pT3 and pT4a colon cancer. (a) Patients were stratified according to elastic laminal invasion (ELI) status. Blue line, ELI-negative cases; red line, ELI-positive cases. (b) Patients were divided into three tumor types. Blue line, ELI-negative type; green, non-elevated type ELI-positive cases; yellow line, elevated type ELI-positive cases.

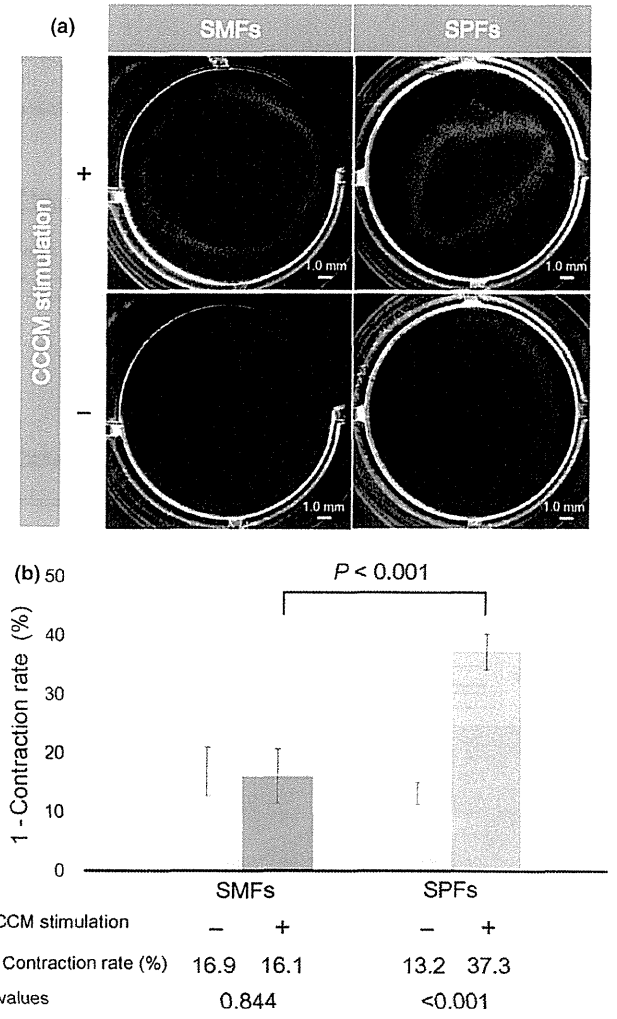

Fig. 6. Contraction assays using submucosal fibroblasts (SMFs) and subperitoneal fibroblasts (SPFs). Gels containing SMFs or SPFs were compared by the presence or absence of cancer cell-conditioned medium (CCCM). (a) Pictures of each gel were taken 48 h after release of each gel from the sides of wells. (b) Contraction rate is shown by bar graph indicating the average value of three gels.

sion was found in CC tissue with strictures and enhanced contractile ability of fibroblasts.[20–22] Concordant with these previous studies, we also found a robust functional contractile ability of SPFs that seemed to be associated with the bowel obstruction. In addition, the spread of CMPI may contribute to the development of clinical findings related to bowel obstruction. However, the spread of this microenvironment did not deteriorate the patient's prognosis. Consequently, the tumor biology would have been already altered by the formation of CMPI, and the spread of CMPI would lead to alteration of tumor morphology.

Morphological alteration in the course of tumor progression has been studied in the early stage of carcinogenesis, as in adenoma–carcinoma sequences and *de novo* cancer. However, there were few studies on the morphological alteration that accompanied the progression of advanced tumor. Recently, we have reported the morphological alteration associated with ELI-positive type invasion.[6] Further detailed analysis in this study revealed that the elevation of the PEL was strongly associated with lateral tumor spread and the resulting increase in tumor annularity rate, which suggested that the spread of CMPI caused morphological alteration. Based on these findings, we propose a model of the morphological alteration that accompanies progression of advanced CC (Fig. 7).

Understanding stromal events may be helpful in the treatment of CRC. More recent research suggests that tumor stroma might be a good target for therapeutic interventions, in particular chemotherapy.[15] For example, it was reported that treatment of pancreatic cancer with nab-paclitaxel reduced the number of cancer-associated fibroblasts in the cancer stroma and improved the response to chemotherapy.[23] Twenty-five percent of patients with uncomplicated CRC with unresectable distant metastasis who underwent chemotherapy required palliative intervention such as bypass surgery, colonic stent, and palliative resection; approximately 80% of these interventions were due to colonic obstruction.[24] We speculate that treatment for tumor stroma improves bowel patency, thereby avoiding stent placement or palliative surgeries that are required for bowel obstruction. Treatments for tumor stroma may be effective in treating patients with unresectable primary CRC to avoid invasive palliative procedures.

The limitation of our study is that there is a difference in the number of H&E and elastica stained slides examined in each case, because we could not adopt the protocol with a predefined number of blocks and sections due to the priority on clinical diagnosis. This might cause a bias in the classification of tumor types.

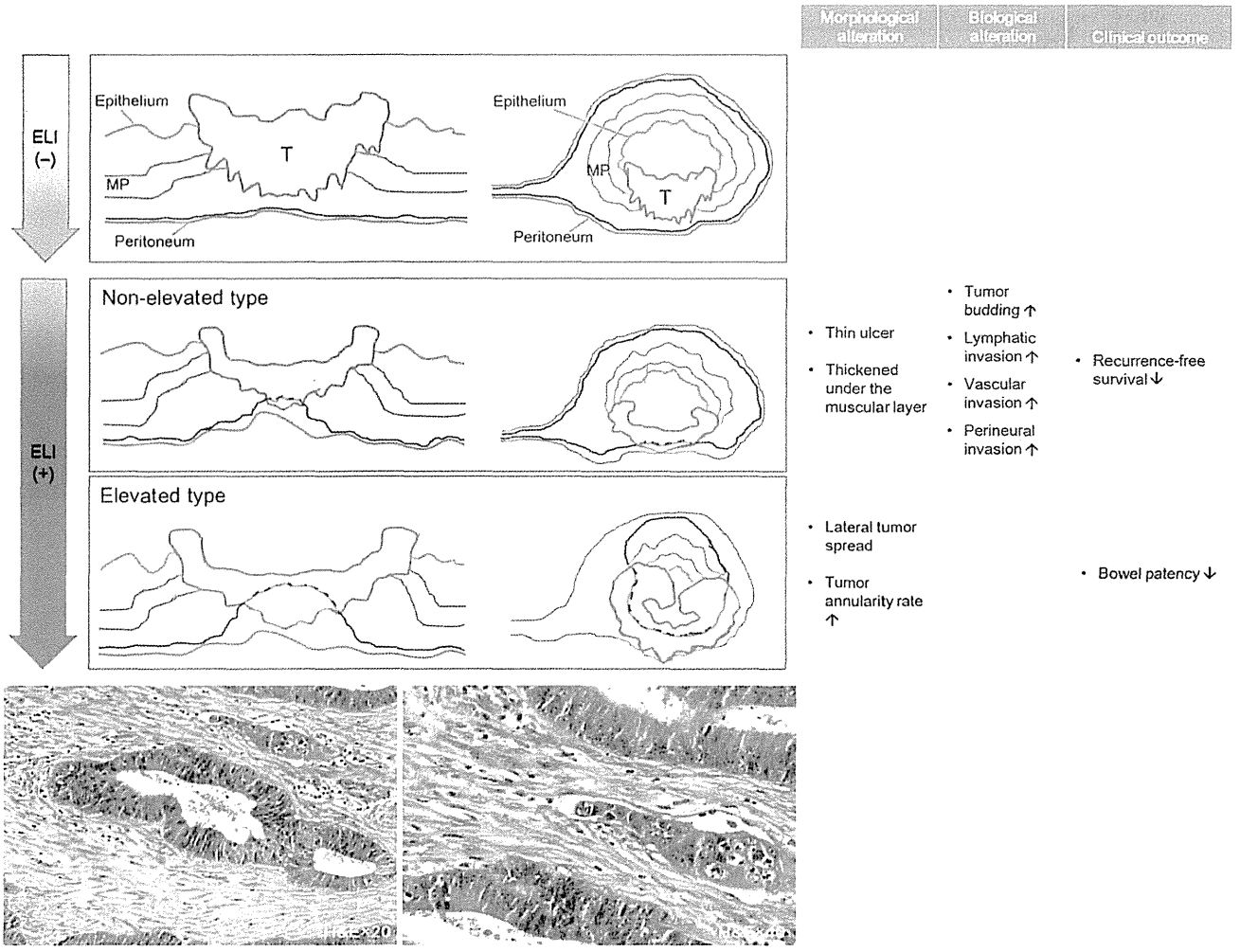

Fig. 7. Proposed model for the tumor progression of colon cancer. Tumor progressed in order of elastic laminal invasion (ELI)-negative type, non-elevated type ELI-positive cases, and elevated type ELI-positive cases. Associations between tumor progression phase and morphological alterations, and biological alterations are described, and the resulting clinical features are shown. The red line represents the peritoneal elastic lamina, and the area filled with yellow represents the cancer microenvironment formed by peritoneal invasion. Histological features of the latter are abundant spindle-shaped fibroblasts and collagen. Higher magnification more clearly revealed spindle-shaped fibroblasts. MP, muscularis propria; T, tumor.

In conclusion, the tumor-promoting microenvironment of CMPI spread into the luminal side of the colonic wall after ELI, and caused bowel obstruction through activation of SPFs. The clinical outcome was affected by CMPI formation, and clinical findings were affected by the spread of CMPI. We are the first group to show that the tumor-promoting microenvironment can spread in the course of tumor progression and can influence physical findings.

Acknowledgment

This study was supported by grants from the Japan Society for the Promotion of Science (Kakenhi 24590458).

Disclosure Statement

The authors have no conflict of interest.

References

1 Ferlay J, Parkin DM, Steliarova-Foucher E. Estimates of cancer incidence and mortality in Europe in 2008. *Eur J Cancer* 2010; **46**: 765–81.
2 Jemal A, Bray F, Center MM, Ferlay J, Ward E, Forman D. Global cancer statistics. *CA Cancer J Clin* 2011; **61**: 69–90.
3 Siegel R, Naishadham D, Jemal A. Cancer statistics, 2012. *CA Cancer J Clin* 2012; **62**: 10–29.
4 Majumdar SR, Fletcher RH, Evans AT. How does colorectal cancer present? Symptoms, duration, and clues to location. *Am J Gastroenterol* 1999; **94**: 3039–45.
5 Hamilton W, Round A, Sharp D, Peters TJ. Clinical features of colorectal cancer before diagnosis: a population-based case–control study. *Br J Cancer* 2005; **93**: 399–405.
6 Kojima M, Nakajima K, Ishii G, Saito N, Ochiai A. Peritoneal elastic laminal invasion of colorectal cancer: the diagnostic utility and clinicopathologic relationship. *Am J Surg Pathol* 2010; **34**: 1351–60.
7 Liang WY, Chang WC, Hsu CY *et al.* Retrospective evaluation of elastic stain in the assessment of serosal invasion of pT3N0 colorectal cancers. *Am J Surg Pathol* 2013; **37**: 1565–70.

8 Yokota M, Kojima M, Nomura S *et al.* Clinical impact of elastic laminal invasion in colon cancer: elastic laminal invasion-positive stage II colon cancer is a high-risk equivalent to stage III. *Dis Colon Rectum* 2014; **57**: 830–8.
9 Kojima M, Higuchi Y, Yokota M *et al.* Human subperitoneal fibroblast and cancer cell interaction creates microenvironment that enhances tumor progression and metastasis. *PLoS One* 2014; **9**: e88018.
10 Sobin LH, Gospodarowicz MK, Wittekind C, eds. *TNM Classification of Malignant Tumors*, 7th edn. West Sussex, UK: Wiley-Blackwell, 2009.
11 Ngo P, Ramalingam P, Phillips JA, Furuta GT. Collagen gel contraction assay. *Methods Mol Biol* 2006; **341**: 103–9.
12 Ueyama T, Yao T, Nakamura K, Enjoji M. Obstructing carcinomas of the colon and rectum: clinicopathologic analysis of 40 cases. *Jpn J Clin Oncol* 1991; **21**: 100–9.
13 Miura S, Kodaira S, Hosoda Y. Immunohistologic analysis of the extracellular matrix components of the fibrous stroma of human colon cancer. *J Surg Oncol* 1993; **53**: 36–42.
14 Miyamoto S, Boku N, Fujii T *et al.* Macroscopic typing with wall stricture sign may reflect tumor behaviors of advanced colorectal cancers. *J Gastroenterol* 2001; **36**: 158–65.
15 Lorusso G, Ruegg C. The tumor microenvironment and its contribution to tumor evolution toward metastasis. *Histochem Cell Biol* 2008; **130**: 1091–103.
16 Alphonso A, Alahari SK. Stromal cells and integrins: conforming to the needs of the tumor microenvironment. *Neoplasia* 2009; **11**: 1264–71.
17 Hanahan D, Weinberg RA. Hallmarks of cancer: the next generation. *Cell* 2011; **144**: 646–74.
18 Quail DF, Joyce JA. Microenvironmental regulation of tumor progression and metastasis. *Nat Med* 2013; **19**: 1423–37.
19 Schmitt-Graff A, Desmouliere A, Gabbiani G. Heterogeneity of myofibroblast phenotypic features: an example of fibroblastic cell plasticity. *Virchows Arch* 1994; **425**: 3–24.
20 Tomasek JJ, Gabbiani G, Hinz B, Chaponnier C, Brown RA. Myofibroblasts and mechano-regulation of connective tissue remodelling. *Nat Rev Mol Cell Biol* 2002; **3**: 349–63.
21 Otranto M, Sarrazy V, Bonte F, Hinz B, Gabbiani G, Desmouliere A. The role of the myofibroblast in tumor stroma remodeling. *Cell Adh Migr* 2012; **6**: 203–19.
22 Hinz B. Matrix mechanics and regulation of the fibroblast phenotype. *Periodontol 2000* 2013; **63**: 14–28.
23 Alvarez R, Musteanu M, Garcia-Garcia E *et al.* Stromal disrupting effects of nab-paclitaxel in pancreatic cancer. *Br J Cancer* 2013; **109**: 926–33.
24 Yun JA, Park Y, Huh JW *et al.* Risk factors for the requirement of surgical or endoscopic interventions during chemotherapy in patients with uncomplicated colorectal cancer and unresectable synchronous metastases. *J Surg Oncol* 2014; **110**: 839–44.

J Gastroenterol (2014) 49:400–407
DOI 10.1007/s00535-013-0822-1

The Japanese Society of Gastroenterology

ORIGINAL ARTICLE—ALIMENTARY TRACT

Histogenesis and prognostic value of myenteric spread in colorectal cancer: a Japanese multi-institutional study

Hideki Ueno · Kazuo Shirouzu · Hideyuki Shimazaki · Hiroshi Kawachi · Yoshinobu Eishi · Yoichi Ajioka · Kiyotaka Okuno · Kazutaka Yamada · Toshihiko Sato · Takaya Kusumi · Ryoji Kushima · Masahiro Ikegami · Motohiro Kojima · Atsushi Ochiai · Akihiko Murata · Yoshito Akagi · Takahiro Nakamura · Kenichi Sugihara · Study Group for Perineural Invasion projected by the Japanese Society for Cancer of the Colon and Rectum (JSCCR)

Received: 14 February 2013 / Accepted: 28 March 2013 / Published online: 16 May 2013

Abstract
Background The histogenesis of the pattern of cancer spread along Auerbach's plexus (myenteric spread: MS) remains unclear and its prognostic value in colorectal cancer (CRC) has not been thoroughly investigated.
Methods Pathology slides of 2845 pT2/pT3/pT4 CRCs stained with hematoxylin–eosin (H&E) were reviewed at 10 institutions. MS was classified into 2 groups depending on whether it was accompanied by the finding of perineural invasion (PN) within the lesion. In addition, immunohistochemical staining (D2-40, S100, CD56, synaptophysin) was performed for serially sectioned specimens from 50 CRCs diagnosed as having PN-negative MS.
Results MS was observed in 504 patients (17.7 %); 360 patients were classified as having PN-positive MS and 144 as having PN-negative MS. The 5-year disease-free survival rate of patients with MS was lower than that of patients without MS (63.3 vs 82.7 %, $P < 0.0001$); however, there was no significant difference in survival outcome according to the presence or absence of intralesion PN in MS. Multivariate analysis showed that the prognostic impact of MS was independent of conventional prognosticators including T and N stages, vascular invasion and extramural PN. In all the tumors having PN-negative MS, remnants of neural tissue were identified within or around cancer nests located at the leading edge of MS.
Conclusions MS is an important prognostic factor for CRC. This feature is the result of cancer development with replacement of Auerbach's plexus and can be classified as intramural PN. The clinical significance of "Pn1" in the UICC/AJCC TNM classification could be enhanced by individual assessment both intramurally and extramurally.

H. Ueno (✉)
Department of Surgery, National Defense Medical College, 3-2 Namiki, Tokorozawa, Saitama 359-8513, Japan
e-mail: ueno@ndmc.ac.jp

K. Shirouzu · Y. Akagi
Department of Surgery, Kurume University Faculty of Medicine, Kurume, Japan

H. Shimazaki
Department of Laboratory Medicine, National Defense Medical College, Tokorozawa, Japan

H. Kawachi · Y. Eishi
Department of Human Pathology, Tokyo Medical and Dental University, Tokyo, Japan

Y. Ajioka
Division of Molecular and Diagnostic Pathology, Graduate School of Medical and Dental Sciences, Course for Molecular and Cellular Medicine, Niigata University, Niigata, Japan

K. Okuno
Department of Surgery, Kinki University School of Medicine, Osakasayama, Japan

K. Yamada
Department of Surgery, Coloproctology Center, Takano Hospital, Kumamoto, Japan

T. Sato
Department of Surgery, Yamagata Prefectural Central Hospital, Yamagata, Japan

T. Kusumi
Department of Surgery, Keiyukai Sappro Hospital, Sapporo, Japan

R. Kushima
Department of Pathology, National Cancer Center Hospital, Tokyo, Japan

Keywords Colorectal cancer · Myenteric spread · Auerbach's plexus · Perineural invasion · The UICC/AJCC TNM classification

Introduction

Perineural invasion (PN) has long been recognized as a clinically important pathological feature of various malignant tumors and is strongly associated with adverse prognostic outcome [1]. In the 7th edition of TNM Classification of Malignant Tumours, the designations of "Pn0" and "Pn1" are applied for tumors with no PN and those with PN, respectively [2]. In the field of colorectal cancer (CRC), the American Joint Committee on Cancer (AJCC) staging manual (seventh edition) recommends PN be recorded as a site-specific prognostic marker in CRC [3]. However, the bowel layer for PN assessment is not clearly referenced, and the assessment of intramural PN in routine pathological practice presumably varies depending on both the institutions and pathologist involved.

Regarding the distribution of intramural PN, it is rarely observed in the submucosal, circular muscle, or longitudinal muscle layers in CRC; however, intramural PN foci are practically observed in the Auerbach's plexus area. Although few studies have investigated the clinical value of PN in Auerbach's plexus, a prospective single-institutional study demonstrated that a distinctive pattern of horizontal cancer spread along the Auerbach's plexus area (myenteric spread) accompanied by PN was associated with adverse prognostic outcome [4]. In addition, myenteric spread was shown to be associated with unfavorable prognostic outcome, irrespective of intralesion PN findings [5].

The actual histogenesis of myenteric spread has not been clarified to date. Although pre-existing structures such as local neural or lymphatic networks may be considered original structures very relevant to this type of cancer development, histological evidence of the tumor utilizing a specific pre-existing structure as a development route has not been consistently detected in lesions. Therefore, whether myenteric spread simply results from a single histogenesis, e.g., PN, or is multifactorial remains unclear.

This multi-institutional study was projected by the Japanese Society for Cancer of the Colon and Rectum (JSCCR) for establishing assessment criteria for determining PN in CRC. In this study, we attempted to clarify the underlying histogenesis of myenteric spread on the basis of prognostic and immunohistochemical analyses and to clarify the clinical implication of this type of cancer spread.

Patients and methods

Patients

In total, 2845 patients with pT2/pT3/pT4 CRC who consecutively underwent curative surgery at 10 JSCCR institutions (Kurume University Faculty of Medicine, National Defense Medical College, Tokyo Medical and Dental University, Takano Hospital, Keiyukai Sapporo Hospital, National Cancer Center Hospital, Jikei University School of Medicine, Hirosaki University School of Medicine, Kinki University School of Medicine, and Yamagata Prefectural Central Hospital) between 1999 and 2004 were analyzed. This dataset included 1695 men and 1150 women (average age 65 years, range 17–96 years). No patient received preoperative chemotherapy or radiotherapy. With regard to adjuvant therapy administered to patients, 1113 patients received chemotherapy, 1658 patients received no adjuvant therapy, and little information on postoperative treatment was available for 74 patients. Chemotherapy with single oral anticancer drugs was the most common postoperative therapy administered (765), followed by 5FU/leucovorin (255) and UFT/leucovorin (56). The average follow-up was 77 months (range 1–149 months) for 2151 survivors.

Histological evaluation of myenteric cancer spread

The pattern of horizontal cancer spread along the Auerbach's plexus zone was defined as myenteric spread (Fig. 1). Myenteric spread was assessed on hematoxylin–eosin (H&E) slides prepared in routine pathological practice and was classified into 2 types depending on whether the lesion was accompanied by the histological finding of PN. PN was defined as the histological finding of tumor cells invading or spreading along nerve fascicles. The status of myenteric spread as well as PN

M. Ikegami
Department of Pathology, Jikei University School of Medicine, Tokyo, Japan

M. Kojima · A. Ochiai
Pathology Division, Research Center for Innovative Oncology National Cancer Center Hospital East, Kashiwa, Japan

A. Murata
Department of Surgery, Hirosaki University School of Medicine, Hirosaki, Japan

T. Nakamura
Laboratory for Mathematics, National Defense Medical College, Tokorozawa, Japan

K. Sugihara
Department of Surgery, Tokyo Medical and Dental University, Tokyo, Japan

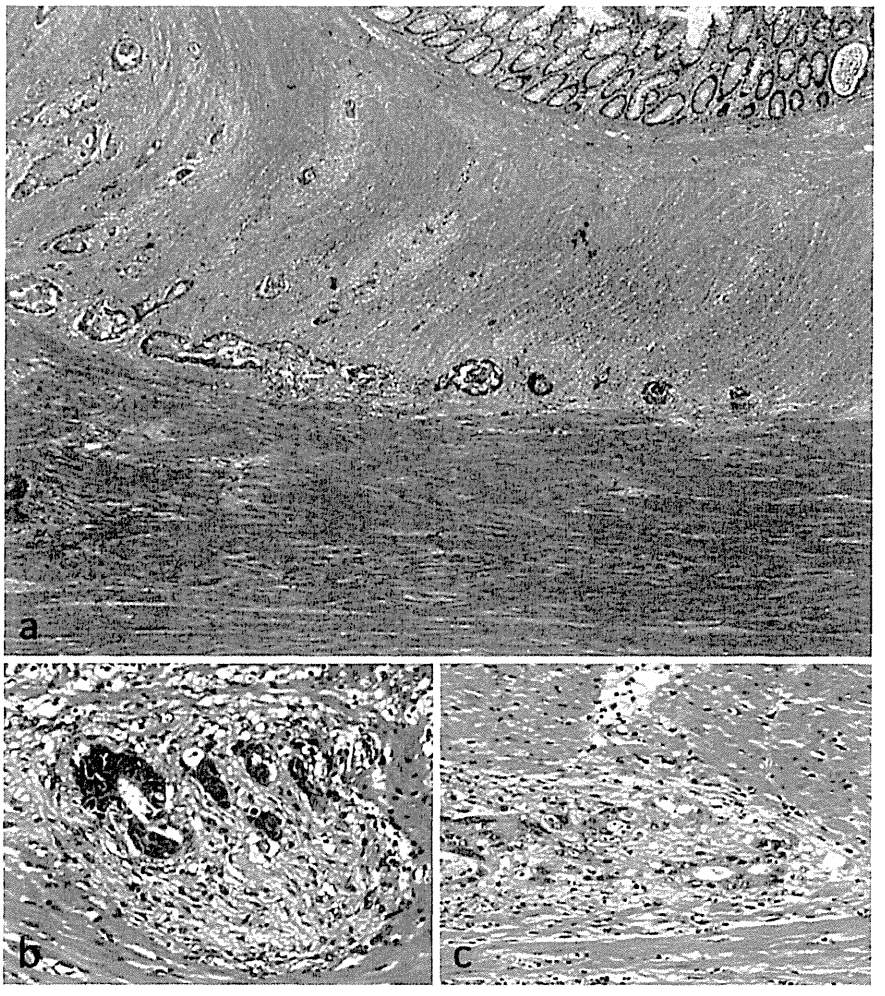

Fig. 1 Myenteric spread in colorectal cancer. **a** Horizontal spread of cancer along the Auerbach's plexus zone was defined as myenteric cancer spread. **b** In a myenteric spread lesion, we observed nerve fascicles associated with cancer cells in certain instances; however, **c** histological findings of neural involvement were not obvious in others. All images, H&E staining (**a** ×4 objective lens; **b**, **c** ×40 objective lens)

external to the muscularis propria (extramural PN) was evaluated at each institution. The consensus for the concept of judging myenteric spread and its classification was kept among institutions participated in this study on the basis of some histological pictures as shown in Fig. 1.

Immunohistochemical staining with neural and lymphatic markers

Serially sectioned slides were prepared from tumors, which had been diagnosed as showing myenteric spread but were unaccompanied by evidence of PN, at 6 institutions (National Defense Medical College, Tokyo Medical and Dental University, Niigata University, Kinki University School of Medicine, Keiyukai Sapporo Hospital, and Yamagata Prefectural Central Hospital). In total, 50 tumors in which myenteric spread was observed (on glass slides newly prepared for immunohistochemical examination) were submitted to the study to clarify the histogenesis of myenteric spread. Immunohistochemical staining was performed on serially sectioned specimens using neural markers (synaptophysin, S100, and CD56) and D2-40 antibody. For tumors in which no positive findings were observed within myenterically spread lesions according to these markers of immunohistochemical staining, serial sectioning and staining were repeatedly performed in the same manner.

Statistical analyses

Correlation between the 2 types of myenteric spread as well as the distribution of myenteric spread and extramural PN was evaluated by the Chi-square test and the *t* test. The disease-free and overall survival rates were calculated on the basis of the Kaplan–Meier method, and differences assessed by the log-rank test. Cox proportional hazards regression analysis was used to determine the impact of prognostic parameters on disease-free survival. Statistical calculations were performed using StatView ver. 5.0 software (SAS Institute, Cary, NC, USA) and SPSS software package (SPSS, Inc., Chicago, IL, USA).

Results

Incidence and prognostic impact of myenteric spread

Myenteric spread was observed in 504 patients (17.7 %). It was significantly associated with T and N stages as well as with conventional histological parameters such as tumor differentiation, lymphatic invasion, venous invasion, and extramural PN (Table 1).

The incidence of myenteric spread differed according to the location of the primary tumor (Fig. 2). The incidence of myenteric spread was lower in the cecum and lower rectum than in other parts of the large bowel. In contrast, the incidence of extramural PN was higher in the rectum than in the colon.

Myenteric spread exerted a significant adverse effect on postoperative disease-free survival and overall survival (Fig. 3). Multivariate Cox proportional analysis showed that the prognostic impact of myenteric spread was independent of conventional prognostic markers including tumor differentiation, T stage, N stage, vascular invasion and extramural PN (Table 2).

Comparison of myenteric spread in relation to evidence of intralesion PN

Among tumors showing myenteric spread, 360 tumors had evidence of PN in the myenteric spread lesion on H&E slides, whereas such finding could not be observed in 144 tumors. Conventional parameters associated with metastatic potential such as N status, tumor grade, vascular invasion, and extramural PN did not differ according to the presence of PN in lesions with myenteric spread, although myenteric spread with positive evidence of PN was less frequently detected in larger tumors and in those invading the deeper layers (Table 1). Tumor

Table 1 Clinicopathological background of tumors showing myenteric spread

	Overall ($N = 2845$)			Tumors with myenteric spread ($N = 504$)		
	Myenteric spread			Finding of PN on H&E slides		
	Absence (2341)	Presence (504)	P value	Absence (144)	Presence (360)	P value
Gender						
Male	1390 (82.0)	305 (18.0)	0.6363	86 (28.2)	219 (71.8)	0.8177
Female	951 (82.7)	199 (17.3)		58 (29.1)	141 (70.9)	
Tumor location						
Right colon	671 (84.7)	121 (12.3)	0.0001	40 (33.1)	81 (66.9)	0.2551
Left colon	949 (78.8)	256 (21.2)		74 (28.9)	182 (71.1)	
Rectum	721 (85.0)	127 (15.0)		30 (23.6)	97 (76.4)	
Tumor diameter	49.2	48.8	0.7870	51.7	47.7	0.0475
T stage						
T2	525 (95.3)	26 (4.7)	<0.0001	4 (15.4)	22 (84.6)	0.0040
T3	1370 (81.1)	320 (18.9)		80 (25.0)	240 (75.0)	
T4	446 (73.8)	158 (26.2)		60 (38.0)	98 (62.0)	
N stage						
N0	1478 (88.5)	192 (11.5)	<0.0001	65 (33.9)	127 (66.1)	0.1166
N1	664 (76.4)	205 (23.6)		51 (24.9)	154 (75.1)	
N2	199 (65.0)	107 (35.0)		28 (26.2)	79 (73.8)	
No. of LN examined	24.6	24.6	0.9384	24.9	24.5	0.8182
Tumor differentiation						
G1	1143 (84.9)	203 (15.1)	0.0010	61 (30.0)	142 (70.0)	0.1592
G2	1047 (79.4)	271 (20.6)		79 (29.2)	192 (70.8)	
G3	151 (83.4)	30 (16.6)		4 (13.3)	26 (86.7)	
Lymphatic invasion						
Negative	836 (90.0)	93 (10.0)	<0.0001	26 (28.0)	67 (72.0)	0.8845
Positive	1505 (78.5)	411 (21.5)		118 (28.7)	293 (71.3)	
Venous invasion						
Negative	987 (84.9)	176 (15.1)	0.0027	49 (27.8)	127 (72.2)	0.7903
Positive	1354 (80.5)	328 (19.5)		95 (29.0)	233 (71.0)	
Extramural PN						
Negative	2177 (86.0)	353 (14.0)	<0.0001	99 (28.2)	254 (72.0)	0.6893
Positive	164 (52.1)	151 (47.9)		45 (29.4)	106 (70.2)	

PN perineural invasion, *H&E* hematoxylin and eosin, *LN* lymph node

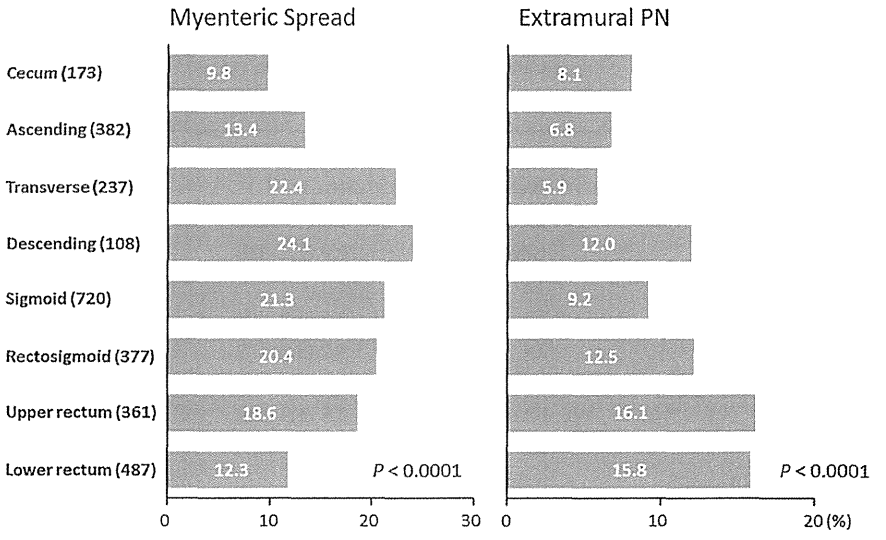

Fig. 2 Incidence of myenteric spread and extramural perineural invasion (PN) according to location of the primary tumor

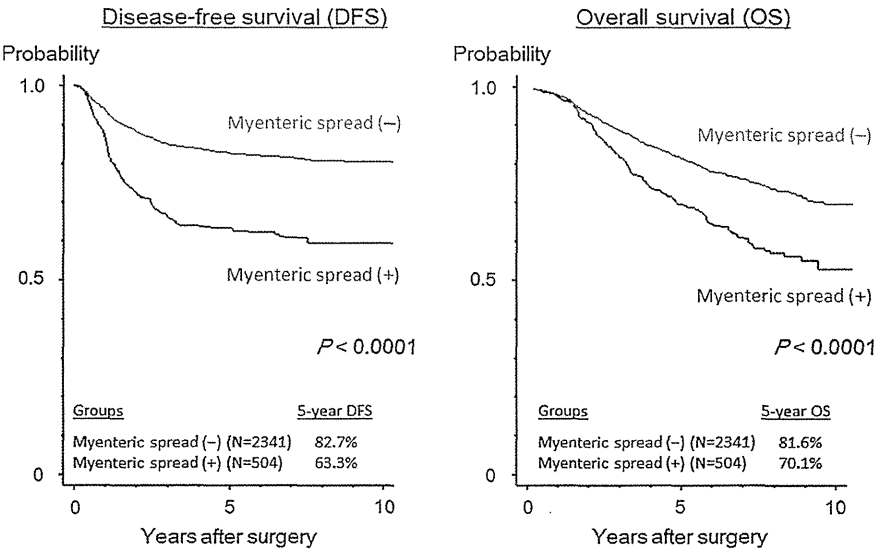

Fig. 3 Disease-free and overall survival curves with or without myenteric spread in colorectal cancer

location was also found to be unrelated to the type of myenteric spread.

With regard to prognostic relevance, there was no significant difference in the recurrence-free and overall survival rate of patients with myenteric spread in relation to the intralesion presence or absence of PN.

Immunohistochemical staining for myenteric spread

In 48 out of 50 tumors, immunohistochemical staining using neural markers revealed the existence of remnants of neural tissue within or around cancer nests (Fig. 4) located at the leading edge of myenteric spread. For 2 tumors showing negative result, additional sectioning followed by immunohistochemical staining was performed in the same manner as that performed previously, and in both the cases, a remnant of neural tissue was observed in a cancer nest located at the leading edge of the myenteric spread. Consequently, in all the 50 tumors diagnosed by H&E staining as showing myenteric spread but unaccompanied by PN, a positive result was obtained with regard to the finding of nerve involvement by the tumor.

On the other hand, on the basis of D2-40 immunostaining, cancer foci within lymphatic channels in the Auerbach's plexus area were observed only in 2 cases. Both these tumor foci were located at the center of the lesion.

Discussion

With regard to the underlying histogenesis of myenteric spread in CRC, histological evidence of PN was identified

Table 2 Univariate and multivariate analyses of disease-free survival by the Cox proportional hazards regression model

Variables	Category	Univariate		Multivariate	
		HR (95 % CI)	*P* value	HR (95 % CI)	*P* value
Tumor size (mm)		1.0 (1.0–1.0)	<0.0001	–	
Tumor differentiation	Well	1		1	
	Moderate	1.8 (1.5–2.2)	<0.0001	1.3 (1.1–1.6)	0.0041
	Others	2.9 (2.2–3.9)	<0.0001	2.0 (1.5–2.7)	<0.0001
T stage	T2	1		1	
	T3	2.6 (1.9–3.5)	<0.0001	1.7 (1.2–2.3)	0.0008
	T4	4.2 (3.0–5.7)	<0.0001	2.2 (1.6–3.0)	<0.0001
N stage	N0	1		1	
	N1	2.3 (1.9–2.8)	<0.0001	2.1 (1.7–2.5)	<0.0001
	N2	5.6 (4.6–6.9)	<0.0001	3.4 (2.7–4.3)	<0.0001
Lymphatic invasion	Negative	1		–	
	Positive	2.0 (1.6–2.4)	<0.0001		
Venous invasion	Negative	1		1	
	Positive	1.8 (1.5–2.1)	<0.0001	1.4 (1.2–1.7)	0.0001
Myenteric spread	Negative	1		1	
	Positive	2.4 (2.0–2.9)	<0.0001	1.4 (1.1–1.7)	0.0016
Extramural PN	Negative	1		1	
	Positive	4.2 (3.5–5.0)	<0.0001	2.2 (1.8–2.7)	<0.0001

HR hazard ratio, *CI* confidence interval

without exception at the advancing edge of this distinctive horizontal spread on the basis of immunohistochemical staining with neural markers. On the other hand, the results of D2-40 immunohistochemical staining confounded the hypothesis that cancer development through the lymphatic network is the underlying cause of myenteric spread. In addition, with regard to differences in the clinicopathological background of tumors with myenteric spread according to the presence or absence of intralesion PN, there were no significant differences in conventional factors associated with tumor aggression, such as tumor grade, vascular invasion, extramural PN, or lymph node metastasis. We also observed that there were no differences in prognostic outcome between the 2 tumor groups. All the findings of our study indicate that myenteric spread in CRC is the result of a single histogenesis, PN, i.e., cancer development with the replacement of the nerves of Auerbach's plexus, and this type of cancer spread is intrinsically the same, irrespective of whether PN is identified on H&E slides.

Some authors regard the nerve sheath as important in the assessment criteria of PN [1, 6, 7]. Fujita et al. [4] defined PN in Auerbach's plexus as the presence of cancer nests inside the perineurium. However, it is difficult to identify the perineurium in Auerbach's plexus on H&E slides. We believe that myenteric spread should be recognized as intramural PN, irrespective of whether cancer nests are located within the perineurium. The standard of this assessment criterion allows pathologists to diagnose intramural PN without special additional staining to identify the perineurium, and improvement in interobserver agreement in determining intramural PN may thus be expected.

There is much literature concerning extramural PN in CRC [6, 8–13], which is repeatedly shown as an independent prognostic indicator [10, 11, 14–17] and the National Comprehensive Cancer Network (NCCN) guidelines regard PN as a high-risk factor for recurrence in stage II patients [18]. However, the actual status and clinical value of intramural PN have not been fully investigated. It is noteworthy that intramural PN (i.e., myenteric spread) was demonstrated to impact survival outcome independent of conventional parameters including stage-factors and extramural PN in the present study.

We found fundamental differences between intramural PN and extramural PN. First, distribution within the large bowel varies greatly. The incidence of PN is reportedly higher in rectal cancer than in colon cancer [12]. This appeared to be the case for extramural PN in our study, although the incidence of intramural PN was relatively low in the lower rectum and cecum. Second, the survival impact differed between intramural PN and extramural PN, i.e., extramural PN exerted a greater adverse survival impact than intramural PN. Although both the AJCC staging manual and NCCN guidelines treat PN in all layers of the bowel equally as an unfavorable prognostic marker, the clinical value of this site-specific prognostic marker

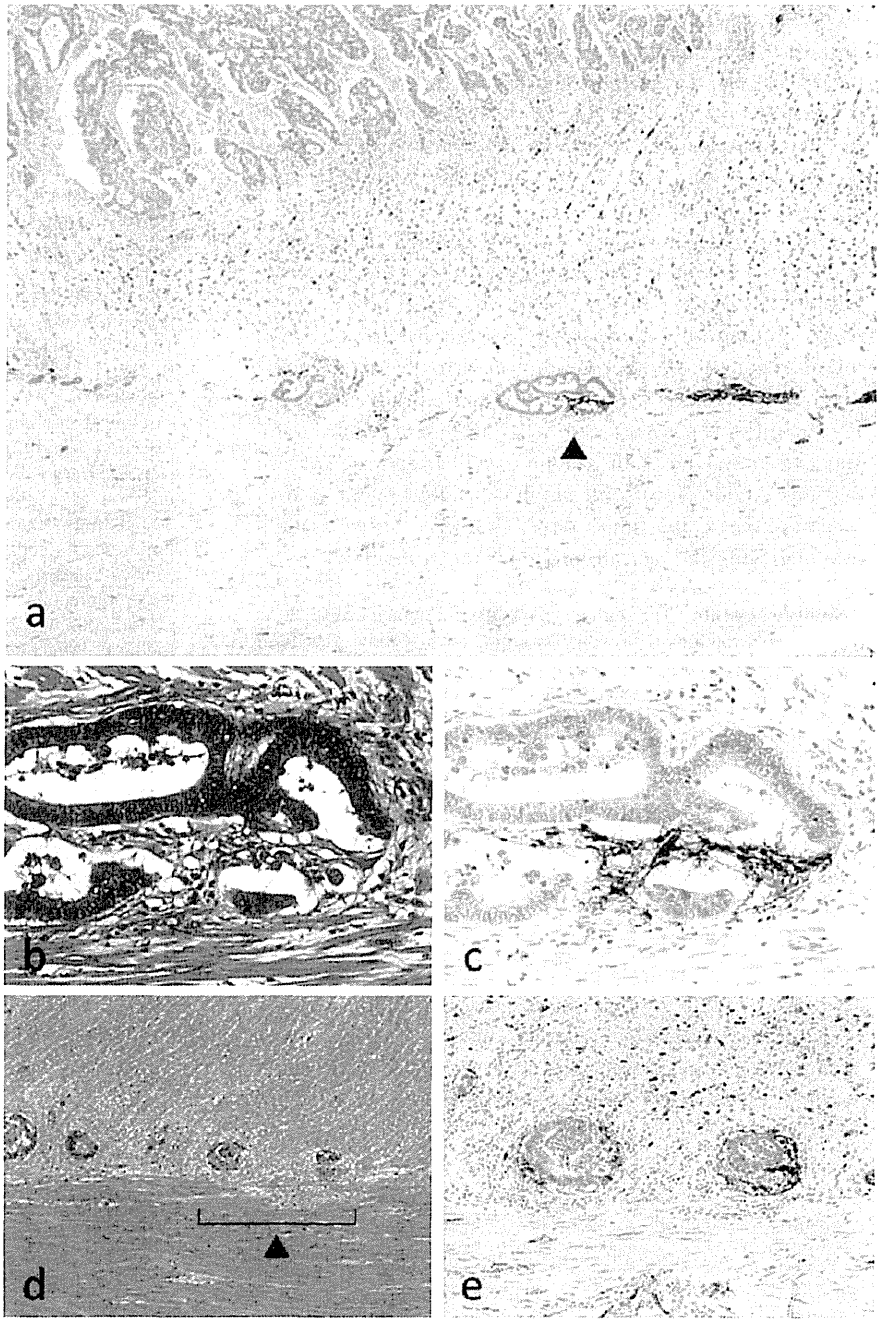

Fig. 4 Serial sectioning of a cancer nest located at the leading edge of myenteric spread. Note that remnant neural tissue exists within or around a cancer nest located at the leading edge of horizontal spread along Auerbach's plexus. **a** S100 immunostaining (×4 objective lens); **b** magnification of area indicated by arrowhead in **a**, H&E staining (×40 objective lens); **c** magnification of area indicated by arrowhead in **a**, S100 immunostaining (×40 objective lens); **d** H&E staining (×10 objective lens); **e** magnification of area indicated by arrowhead in **d**, S100 immunostaining (×20 objective lens)

would be enhanced by discriminating between intramural PN and extramural PN.

Third, there was a difference in the morphological pattern of tumor nerve involvement between intramural PN and extramural PN. In extramural PN foci, cancer nests were located along the nerve fascicles. Generally, we can easily identify nerve fascicles by cancer nests. On the other hand, in myenterically spread lesions (mostly at the advancing edge of horizontal spread), we often observe a "moth-eaten" appearance of the nerves involved, in which tiny cancer nests invade nerve fascicles. This morphological pattern leads us to a presumption that cancer develops by replacing nerve tissue, resulting in its disappearance, and this is why the typical finding of PN is rarely observed in myenterically spread lesions, except at the leading edge. Two types of nerve sheath are present in the nervous system distributed within the large bowel: the endoneurium and perineurium. The abovementioned differences in the morphological pattern of nerve involvement by cancer cells between intramural and extramural layers leads us to the

view that myenterically spread tumors may have a greater affinity to the endoneurium or neural fibers in the Auerbach's area, whereas the adhesion of tumor cells to the perineurium plays a key role in the development of PN in the extramural area. Otherwise, the function of the perineurium as a tumor barrier may differ between intramural and extramural areas.

In conclusion, this study clarified that PN in the Auerbach's plexus area is the histogenesis of myenteric spread. Differences in distribution within the large bowel, prognostic impact, and morphology of the pattern of nerve involvement suggest that the molecular background of PN may differ between the intramural and extramural layers. PN should be separately recorded with regard to intramural and extramural areas in routine practice, and we believe that this could offer useful prognostic information as well as contribute to the future development of basic research into clarifying the neurotropic mechanism involved.

Acknowledgments The authors thank the following investigators for their contributions with valuable advice to this study: Masafumi Tanaka, Department of Surgery, Coloproctology Center, Takano Hospital; Shinji Yoshii, Department of Gastroenterology, Keiyukai Sappro Hospital; Tadao Tokoro, Department of Surgery, Kinki University School of Medicine; Takeshi Suto, Department of Surgery, Yamagata Prefectural Central Hospital. This study was funded by the Japanese Society for Cancer of the Colon and Rectum.

Conflict of interest The authors declare no conflict of interest.

References

1. Liebig C, Ayala G, Wiks JA, Berger DH, Albo D. Perineural invasion in cancer. Cancer. 2009;115:3379–91.
2. Sobin LH, Gospodarowicz MK, Wittekind Ch, editors. (International Union Against Cancer). TNM classification of malignant tumours. 7th ed. West Sussex: Wiley-Blackwell; 2009.
3. Edge SB, Byrd DR, Compton CC, Fritz AG, Greene FL, Trotti A, editors. AJCC cancer staging manual (Seventh edition). New York: Springer; 2009.
4. Fujita S, Nakanishi Y, Taniguchi H, Yamamoto S, Akasu T, Moriya Y, et al. Cancer invasion to Auerbach's plexus is an important prognostic factor in patients with pT3–pT4 colorectal cancer. Dis Colon Rectum. 2007;50:1860–6.
5. Ueno H, Hase K, Hashiguchi Y, Ishiguro M, Kajiwara Y, Shimazaki H, et al. Growth pattern in the muscular layer reflects the biological behaviour of colorectal cancer. Colorectal Dis. 2009;11:951–9.
6. Shirouzu K, Isomoto H, Kakegawa T. Prognostic evaluation of perineural invasion in rectal cancer. Am J Surg. 1993;165(2):233–7.
7. Peng J, Sheng W, Huang D, Venook AP, Xu Y, Guan Z, et al. Perineural invasion in pT3N0 rectal cancer. Cancer. 2011;117:1415–21.
8. Seefeld PH, Bargen JA. The spread of carcinoma of the rectum: invasion of lymphatics, vein and nerves. Ann Surg. 1943;118:76–90.
9. Bognel C, Rekacewicz C, Mankarios H, Pignon JP, Elias D, Duvillard P, et al. Prognostic value of neural invasion in rectal carcinoma: a multivariate analysis on 339 patients with curative resection. Eur J Cancer. 1995;31A(6):894–8.
10. Ueno H, Hase K, Mochizuki H. Criteria for extramural perineural invasion as a prognostic factor in rectal cancer. Br J Surg. 2001;88:994–1000.
11. Fujita S, Shimoda T, Yoshimura K, Yamamoto S, Akasu T, Moriya Y. Prospective evaluation of prognostic factors in patients with colorectal cancer undergoing curative resection. J Surg Oncol. 2003;84:127–31.
12. Liebig C, Ayala G, Wilks J, Verstovsek G, Liu H, Agarwal NB, et al. Perineural invasion is an independent predictor of outcome in colorectal cancer. J Clin Oncol. 2009;31:5131–7.
13. Huh JW, Kim HR, Kim YJ. Prognostic value of perineural invasion in patients with stage II colorectal cancer. Ann Surg Oncol. 2010;17:2066–72.
14. Guillem JG, Chessin DB, Cohen AF, Shia J, Mazumdar M, Enker W, et al. Long-term oncologic outcome following preoperative combined modality therapy and total mesorectal excision of locally advanced rectal cancer. Ann Surg. 2005;241:829–38.
15. Stewart D, Yan Y, Mutch M, Kodner I, Hunt S, Lowney J, et al. Predictors of disease-free survival in rectal cancer patients undergoing curative proctectomy. Colorectal Dis. 2008;10:879–86.
16. Uehara K, Nakanishi Y, Shimoda T, Taniguchi H, Akasu T, Moriya Y. Clinicopathological significance of microscopic abscess formation at the invasive margin of advanced low rectal cancer. Br J Surg. 2007;94:239–43.
17. Quah H-M, Chou J, Gonen M, Shia J, Schrag D, Landmann RG, et al. Identification of patients with high-risk stage II colon cancer for adjuvant therapy. Dis Colon Rectum. 2008;51:503–7.
18. National Comprehensive Cancer Network. NCCN clinical practice guidelines in oncology-colon cancer (version 2. 2013). http://www.nccn.org/professionals/physician_gls/pdf/colon.pdf (Accessed 20 Nov 2012).

Pathology

Pathology International 2014; **64**: 591–600

doi:10.1111/pin.12213

Original Article

Tumor-size-based morphological features of metastatic lymph node tumors from primary lung adenocarcinoma

Eiji Yamada,[1,2] Genichiro Ishii,[1] Nao Aramaki,[1,2] Keiju Aokage,[2] Tomoyuki Hishida,[2] Junji Yoshida,[2] Motohiro Kojima,[1] Kanji Nagai[2] and Atsushi Ochiai[1]

[1]*Division of Pathology, Research Center for Innovative Oncology and* [2]*Division of Thoracic Surgery, National Cancer Center Hospital East, Chiba, Japan*

Most primary lung adenocarcinomas show histological diversity, however, histological diversity in the metastatic lymph node tumors (LNT) is not well defined. The aim of this study was to explore the histological characteristics of the metastatic LNT based on their sizes. We analyzed 163 primary tumors and 509 metastatic LNTs. When the primary tumor showed papillary-predominant subtype, the most frequent histological subtype in the metastatic LNT that were ≤2 mm in diameter was solid subtype (49%), followed by papillary subtype (35%); on the other hand, in the metastatic LNT measuring >2 mm in size, the frequency of tumors showing papillary-predominant subtype increased significantly to 52% ($P = 0.04$). When the primary tumor showed acinar-predominant subtype, the most predominant subtype in the ≤2 mm metastatic LN tumors was acinar subtype (55%), followed by solid subtype (40%), with the frequency of acinar subtype increasing significantly to 76% in the metastatic LNT that were >2 mm in diameter ($P = 0.04$). These results indicate that solid subtype is the characteristic histological subtype in the early phase of the LN metastatic process, and that as the metastatic LNT grow larger, they develop morphological features resembling those in the primary tumor.

Key words: diversity, lung adenocarcinoma, lymph node metastasis, micrometastasis

Adenocarcinoma is the most common histologic type of primary lung cancer and is a major focus of research to improve the patients' survival. In the new adenocarcinoma classification, International Multidisciplinary Lung Adenocarcinoma Classification, published in 2011 by the International Association for the Study of Lung Cancer/American Thoracic Society/European Respiratory Society (IASLC/ATS/ERS), invasive adenocarcinoma is divided into five predominant subtypes: the lepidic-, acinar-, papillary-, micropapillary- and solid-predominant subtypes.[1] Most adenocarcinomas are histologically heterogeneous, consisting of two or more histological subtypes. Matching the new adenocarcinoma classification, many studies have reported the prognosis and characteristics of the gene mutations according to this histological typing.[2–6] However, most previous studies focused on the primary tumors, and few studies have focused on the metastatic lesions.

Metastasis is considered as a complex and multistep process that ultimately results in the formation of a secondary mature tumor.[7–9] At the metastatic site, neoplastic cancer cells first go through an avascular growth phase to reach a size not much more than a few millimeters in diameter. During this phase, a small number of tumor cells survive and interact with the surrounding stromal cells, to then develop into macroscopically detectable metastatic lesions. During this metastatic tumor development, effective and dynamic molecular changes, including the epithelial-mesenchymal transition (EMT) and mesenchymal-epithelial transition (MET) have been reported.[10,11] We previously reported that as intrapulmonary metastatic lesions grow larger, the constituent cancer cells exhibit diverse growth patterns, which results in histological diversity in the secondary tumors, just as in the case of primary tumors.[12] However, the morphological changes in early and small metastatic lymph node tumors have not yet been clarified, and it is not yet known whether larger metastatic lymph node tumors exhibit as much histological diversity as the primary tumors. In the present report, we attempt to elucidate the morphological characteristics of the metastatic lymph nodes with special reference to their size and histological diversity. In the TNM Classification of Malignant Tumors, 7th Edition, published in 2009, for breast cancer, if the size of the cancer spread is larger than 0.2 mm and/or more than 200 cells, but not larger than 2 mm, it is

Correspondence: Genichiro Ishii, MD, PhD, Pathology Division, Research Center for Innovative Oncology, National Cancer Center Hospital East, 6-5-1 Kashiwanoha, Kashiwa, Chiba 277-8577, Japan. Email: gishii@east.ncc.go.jp

Disclosure: None declared.

Received 10 March 2014. Accepted for publication 11 September 2014.

defined as *micrometastasis*.[13] Based on this model, we evaluated the morphological features of metastatic lymph node tumors in relation to their sizes: > 2 mm vs. ≤ 2 mm.

MATERIALS AND METHODS

Patient selection

Lymph node metastasis from primary lung adenocarcinoma was detected in 184 consecutive patients who underwent surgical resection without preoperative therapy at the National Cancer Center Hospital East, Chiba, Japan, between January 2008 and December 2012. After excluding 21 cases for which only incomplete clinical information was available, the remaining 163 cases with 509 metastatic lymph nodes were histologically evaluated. The data collection and analyses were performed with the approval of the institutional review board.

Pathological studies

All surgical specimens were fixed with 10% formalin and embedded in paraffin. The tumors were cut at approximately 5-mm intervals, and serial 4-μm sections were stained with hematoxylin-eosin. The median number of tissue blocks per resected specimen was 25 (range: 10–90). The materials were subsequently reviewed by two pathologists (E.Y and G.I.) to confirm the presence of lymph node metastasis and to assess the histopathological features of both the primary tumors and the metastatic lymph nodes.

Histological subtyping of the primary tumors

Histological subtyping of the primary tumors was based on the IASLC/ATS/ERS International Multidisciplinary Lung Adenocarcinoma Classification published in 2011. The lepidic subtype is defined as growth of neoplastic cells along preexisting alveolar structures. The papillary subtype is defined as growth of glandular cells along central fibrovascular cores. If a tumor shows lepidic growth, but the alveolar spaces are filled with papillary structures, the tumor is classified as the papillary subtype. The acinar subtype is defined by the formation of round to oval-shaped glandular structures with a central luminal space surrounded by tumor cells. A cribriform arrangement is regarded as representing the acinar subtype of adenocarcinoma. The micropapillary subtype is defined as tumor cells growing in papillary tufts lacking fibrovascular cores, which may appear detached and/or connected to the alveolar walls. Ring-like glandular structures floating within the alveolar spaces are also regarded as representing micropapillary components. The solid-predominant subtype is characterized by the appearance of polygonal tumor cells arranged in sheets, lacking the features of any of the other recognizable histologic subtypes of adenocarcinoma.

Comprehensive histologic subtyping was performed through a process in which the percent area occupied by each histopathological subtype present in a tumor was estimated in 10% increments, followed by identification and classification of that tumor according to the histologic subtype. The predominant subtype was defined as the subtype accounting for the largest percent area in a tumor. In this cohort, none of the primary tumors were identified as showing the micropapillary-predominant subtype. The typical appearances of the histological subtypes of the primary tumors are shown in Fig. 1(a,h,o).

Histological subtyping of the metastatic lymph node tumors

Histological subtyping of the metastatic lymph node tumors was performed according to the same classification that was used for the primary tumor, and the predominant subtype was also identified. In the case of small metastatic tumors, isolated and small clusters of tumor cells which lacked clear differentiation into the papillary or acinar pattern were divided into the solid-predominant subtype. Also, as the micropapillary-predominant subtype, characterized by tumor cells growing in papillary tufts lacking a fibrovascular core, frequently coexisted with the papillary component, it was included in the papillary-predominant subtype.

The sizes of the metastatic lymph node tumors were evaluated based on the maximum diameter of the metastatic lesion in the lymph nodes. According to the TNM classification of Malignant Tumors, 7th Edition, published in 2009, we evaluated the morphological features of the metastatic lymph node tumors in relation to their sizes, > 2 mm vs. ≤ 2 mm. The typical appearances of the histological subtypes of the metastatic lymph node tumors are shown in Fig. 1(b–g,i–n,p–s).

Histological diversity according to the sizes of the metastatic tumors

The number of histological subtypes in the metastatic lymph node tumors of the size two groups (≤2 mm vs. >2 mm) was compared statistically according to the number of subtypes in the primary tumor. As the micropapillary subtype was observed in only a very small proportion of cases, and frequently coexisted with the papillary component, it was included in the papillary subtype.

Clinical information

All available clinical information was obtained from the clinical records and reports of the referring physicians. The records were reviewed for the patient age, sex, smoking history, pathological T and N classification, stage, and number of

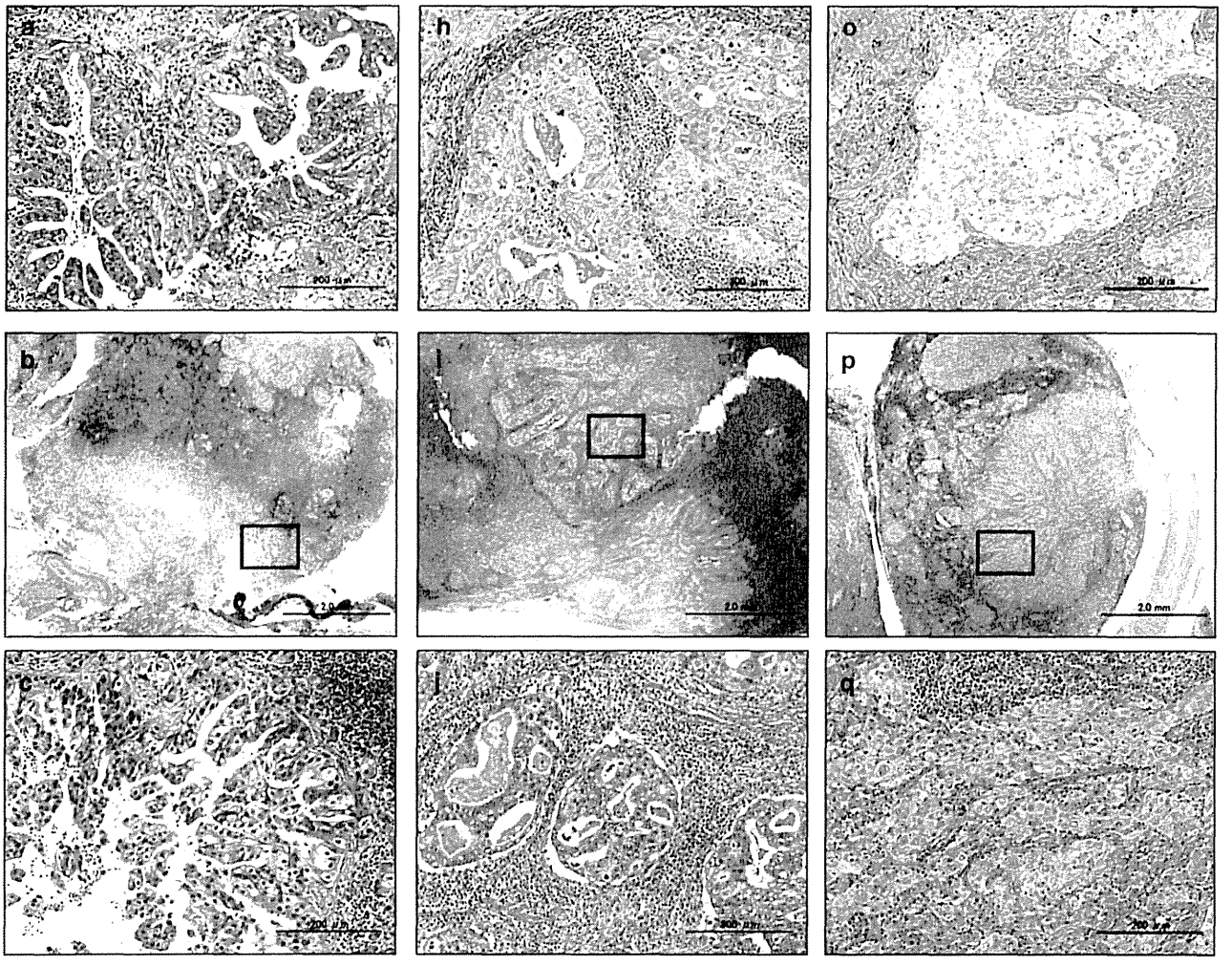

Figure 1 Histopathological features of the primary tumors and metastatic lymph node tumors(H & E). (**a**) Primary tumor showing the papillary-predominant subtype. (**b**) Metastatic lymph node tumor that was >2 mm in diameter. (**c**) Higher magnification view of the tumor shown in **b**. The tumor was mainly composed of the papillary component. (**d,f**) Metastatic lymph node tumors that werre ≤2 mm in diameter. The tumor was mainly composed of the (**d**) solid or the (**f**) papillary component. (**e,g**) Higher magnification views of the tumors shown in **d** and **f**, respectively. (**h**) Primary tumor showing the acinar-predominant subtype. (**i**) Metastatic lymph node tumor that was >2 mm in diameter. (**j**) Higher magnification view of the tumor shown in (**i**). The tumor was mainly composed of the acinar component. (**k**) and (**m**) Metastatic lymph node tumors that were ≤2 mm in diameter. The tumor was mainly composed of the (**k**) solid or the (**m**) acinar component. (**l**) and (**n**) Higher magnification views of the tumors shown in **k** and **m**, respectively. (**o**) Primary tumor showing the solid-predominant subtype. (**p**) and (**r**) Metastatic lymph node tumors that were (**p**) > 2 mm and (**r**) ≤ 2 mm in diameter. (**q**) and (**s**) Higher magnification views of the tumors shown in **p** and **r**, respectively. The tumor was mainly composed of the solid component, irrespective of the tumor size.

metastatic lymph nodes. Pathological staging was based on the TNM classification of the International Union Against Cancer (UICC).[13]

Statistical analysis

Differences in the patient characteristics between the two groups were compared by the Pearson's chi-square test. The unpaired t-test was performed to calculate the statistical significance of the differences. All *P* values are two-sided, and the significance level was set at <0.05. The analyses were performed with the SPSS 11.0 statistical software program (Dr. SPSS II for Windows, standard version 11.0, SPSS Inc., Chicago, IL, USA).

RESULTS

Clinicopathological characteristics of the patients with lymph node metastasis

The clinicopathological characteristics of the 163 adenocarcinoma patients diagnosed as having lymph node metastasis